Uptake of HNO_3 on Hexane and Aviation Kerosene Soots

Ranajit K. Talukdar,*,†,‡ Ekaterina E. Loukhovitskaya,§,|| Olga B. Popovicheva,⊥ and A. R. Ravishankara†,#

National Oceanic and Atmospheric Administration, Earth System Research Laboratory, Boulder, Colorado 80305, Cooperative Institute for Research in Environmental Sciences, University of Colorado, Boulder, Colorado 80309, and Moscow State University, 119992 Moscow, Russia

Received: January 25, 2006; In Final Form: May 11, 2006

The uptake of HNO_3 on aviation kerosene (TC-1) soot was measured as a function of temperature (253−295 K) and the partial pressure of HNO_3, and the uptake of HNO_3 on hexane soot was studied at 295 K and over a limited partial pressure of HNO_3. The HNO_3 uptake was mostly reversible and did not release measurable amounts of gas-phase products such as HONO, NO_3, NO_2 or N_2O_5. The heat of adsorption of HNO_3 on soot was dependent on the surface coverage. The isosteric heats of adsorption, $\Delta^0H^{\text{isosteric}}$, were determined as a function of coverage. $\Delta^0H^{\text{isosteric}}$ values were in the range −16 to −13 kcal mol^{-1}. The heats of adsorption decrease with increasing coverage. The adsorption data were fit to Freundlich and to Langmuir−Freundlich isotherms. The heterogeneity parameter values were close to 0.5, which suggested that a HNO_3 molecule can occupy two sites on the surface with or without being dissociated and that the soot surface could be nonuniform. Surface FTIR studies on the interaction of soot with HNO_3 did not reveal formation of any minor product such as organic nitrate or nitro compound on the soot surface. Using our measured coverage, we calculate that the partitioning of gas-phase nitric acid to black carbon aerosol is not a significant loss process of HNO_3 in the atmosphere.

Introduction

Soot, produced by incomplete combustion of fossil fuels (gasoline, diesel, etc.) and biomass, is ubiquitous in the atmosphere. The role of soot in the atmosphere is varied.[1] Because of its ability to absorb incoming solar radiation,[2] it is expected to heat the atmosphere; this is in contrast to most aerosols that reflect/scatter light and, hence, reduce surface heating. Because soot is only partially oxidized, it can act as a reducing agent by converting oxidized species to their reduced forms. One example is the possible conversion of HNO_3 to NO_2/NO, which has been proposed and is still uncertain. Because it may contain water soluble components and because of its special structure, soot has been proposed by some to be a potential agent for nucleating particles, especially ice;[3−5] others have suggested it to be hydrophobic.[6] It is possible that the method of generation determines the hydrophilicity of soot[7] and is the cause of the diverse conclusions. There are large uncertainties associated with all these proposed influences of soot, and therefore, work on soot is an area of significant research.

Soot is not limited to the lower atmosphere. It has been shown to be present in the upper troposphere and the lower stratosphere (UTLS) region. It has been suggested that the primary source of soot in the UTLS is airplane exhaust,[8−11] and so examinations of the influence of aircraft on climate have paid particular attention to soot.[12,13]

Soot is likely to be altered in the atmosphere via a number of reactions with atmospheric trace species. In particular, because of the co-emission of soot and nitrogen oxides, the interactions between soot and various oxides of nitrogen are of interest. Of special interest is the possible ability of soot to take up HNO_3, both altering the soot surface and regenerating reactive nitrogen oxides. Results from previous studies are in disagreement. Some studies report that HNO_3 uptake by soot is a reversible physical uptake,[14−17] whereas others contend that HNO_3 reacts on the soot surface to regenerate nitrogen oxides[18−22] such as NO_2 and HONO. We will discuss these studies later in the paper. One of the potential reasons for the differences between different studies is that soot is not chemically homogeneous and the variations may arise simply because of variations in the physical and chemical nature of soot due to differences in its sources and in the methods of its production. Therefore, it is of interest to examine various soot samples, especially ones that are close to what is produced in the atmosphere.

In this paper, we present results of HNO_3 uptake on aviation kerosene soot (TC-1) as a function of the gas-phase concentration of HNO_3, $[HNO_3]_g$, and of temperature (253−295 K), and on hexane soot at 295 K and over a limited range of $[HNO_3]_g$. Aviation kerosene was chosen in our experiments because it is a fuel that is burnt in aircraft engines, a major source of soot in the UTLS.[12,23,24] Studies on soot produced by different fuels will help us better understand variation in uptake due to characteristics of soot. We also studied *n*-hexane soot, which has been previously investigated,[14] to provide a comparison. The main aim of this work was to determine if HNO_3 uptake is

* To whom correspondence should be addressed at NOAA. E-mail: Ranajit.K.Talukdar@noaa.gov.

† NOAA, Earth System Research Laboratory, Chemical Sciences Division, R/CSD 2, 325 Broadway, Boulder, CO 80305.

‡ Cooperative Institute for Research in Environmental Sciences, University of Colorado, Boulder, CO 80309.

§ Physics Department, Moscow State University, 11992 Moscow, Russia.

|| Present address: Semenev Institute of Chemical Physics, Russian Academy of Sciences, 4 Kosygin Street, 119991 Moscow, Russia.

⊥ Institute of Nuclear Physics, Moscow State University, 11992 Moscow, Russia.

Also associated with the Department of Chemistry and Biochemistry, University of Colorado, Boulder, CO 80309.

10.1021/jp060556u CCC: $33.50
Published on Web 07/15/2006

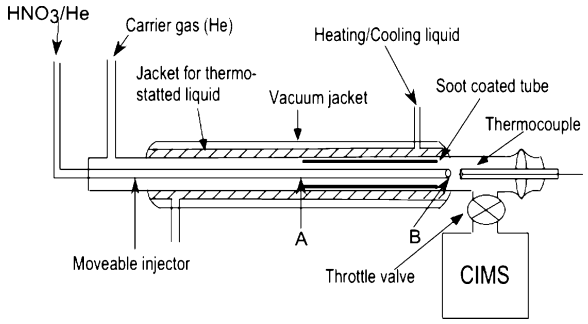

Figure 1. Schematic of the neutral flow tube coupled to the chemical ionization mass spectrometer. The position of the injector tip used to expose soot to HNO_3 is marked A. In position B, the effluents of the injector bypassed the soot sample.

reversible on realistic soot and if uptake leads to the formation of NO_2, HONO, NO_3 or N_2O_5.

Experiments

Two types of experiments were carried out during the course of this study. In one type of experiment, soot-coated tubes placed inside a flow tube equipped with a chemical ionization mass spectrometer (FT-CIMS) was used to measure the uptake of HNO_3 and production of chemically distinct products such as NO_2, HONO, N_2O_5, or NO_3; these constituted the major fraction of experiments. In a few other experiments, a FTIR spectrometer and soot coated on a germanium disk were used to investigate the HNO_3 uptake on the surface and the possible formation of reaction products that are left on the surface. These two types of experiments are described separately below.

Flow Tube-Chemical Ionization Mass Spectrometer (FT-CIMS). The experimental method used to measure the uptake of HNO_3 on two kinds of soot was essentially identical to that used previously in our laboratory to investigate the interaction of HNO_3 and nitrogen oxides on soot.[16,25] Since those studies, the chemical ionization mass spectrometer (CIMS) has been upgraded as described elsewhere.[26] The upgraded apparatus consisted of a flow tube reactor (hereafter referred to as the neutral flow tube, NFT) into which a soot-coated tube (described later) was inserted. HNO_3 was introduced through a movable injector to expose different regions of the soot along the length of the coated tube. The NFT was coupled to an ion flow tube (referred to hereafter as IFT), where ions used to carry out selective ionization, the reagent ions, were generated and allowed to react with molecules of interest. The contents of the gases exiting the IFT, were sampled through a pinhole by a quadrupole mass spectrometer. Details of the IFT and reagent ion generation as well as the measurements of reactive and nonreactive reversible uptake coefficients have been described previously.[16,26]

Neutral Flow Tube (NFT). A schematic of the NFT is shown in Figure 1. The NFT reactor was a 35 cm long double-jacketed Pyrex tube with an internal diameter of 2.0 cm. Thermostated fluid (silicon oil) from a temperature-controlled bath flowed through the inner jacket that was surrounded by an evacuated outer jacket. This arrangement allowed for uniform temperature along the length of the tube and reduced heat loss. The temperature of the flow tube was varied between −50 and +150 °C.

The inside surfaces of 10 cm long cylindrical glass tubes (internal diameter ∼1.8 cm) were coated with soot by suspending the tube in a flame of hexane or aviation kerosene (TC-1 kerosene). The kerosene flame was generated using a lantern. The hexane flame was produced by igniting the vapor over a small amount of hexane in a beaker. An inverted Pyrex funnel was held above the flame of hexane or kerosene. Soot exiting the stem of the funnel was collected on the inside wall of the Pyrex tube.[16,25−27] To ensure uniformity of coating, the Pyrex tube was rotated manually around its cylindrical axis and flipped to introduce the soot stream from both ends.

The effluents of the NFT passed through a Pyrex throttle valve (see Figure 1) into the ion flow tube at a point that was ∼50 cm downstream of the region where reagent ions were produced. The Pyrex throttle valve controlled the gas flow rate out of the NFT. The pressure in the NFT was set by the gas flow rate into and out of the NFT. The pressure in the NFT (2−6 Torr) was significantly higher than that in the IFT (0.2−0.4 Torr). HNO_3 was introduced into the system by flowing ultrahigh purity (UHP) helium over solid HNO_3 kept in a reservoir that was maintained at a constant temperature in the range of 195−213 K. The eluting HNO_3/He mixture was added to the NFT through a 46 cm long, 0.4 cm inner diameter movable Pyrex injector. The position of the injector in the NFT could be varied anywhere along the length of the soot-coated 10 cm long cylinder, which we refer to as the reaction zone. Flow rates of UHP He were between 500 and 1200 STP cm^3 min^{-1} in the NFT and led to linear flow velocities between 800 and 1500 cm s^{-1} through the soot-coated cylinder.

The pressure at the two ends of the NFT was measured with capacitance manometers. A glass tube containing a chromel−alumel thermocouple was inserted from the end opposite to the injector in the flow tube (Figure 1). This thermocouple measured the temperature in the reaction zone under flow conditions identical to those in the experiments. The measured temperature was constant, to within 1 K, along the length of the coated tube. During the uptake measurements, the thermocouple was retracted from the NFT.

The HNO_3 content of the flow tube was measured as the soot-coated tube was being exposed to the gas flow containing HNO_3. The injector was placed at a given position inside the soot-coated tube that defined the length of the coated tube exposed to HNO_3. The time dependence of the HNO_3 signal at this fixed injector position was measured. In addition to changes in HNO_3 signal, other chemically distinct products such as NO_2, HONO, N_2O_5 and NO_3 were monitored simultaneously using CIMS.

Ion Detection Schemes. The reagent ions for chemical ionization, SF_6^- and I^-, were produced by the reactions of thermalized electrons with SF_6 and CF_3I, respectively. A small fraction of the reagent ions reacted with the reactant and product molecules of interest from the NFT to generate the ions that were detected by the quadrupole mass spectrometer. The concentration of the ion produced exclusively from a neutral species of interest was proportional to the product of its concentration and the rate coefficient for its reaction with the reagent ion.

SF_6^- was used as the reagent ion to detect HNO_3, NO_2, HONO and N_2O_5 via the following ion−molecule reactions with rate constants in units of cm^3 $molecule^{-1}$ s^{-1}:[28,29]

$$HNO_3 + SF_6^- \rightarrow NO_3^-\cdot HF + SF_5 \qquad k_1 = 2.0 \times 10^{-9} \quad (1a)$$

$$\rightarrow NO_3^- + \text{product} \quad (1b)$$

$$NO_2 + SF_6^- \rightarrow NO_2^- + SF_6 \qquad k_1 = 1.4 \times 10^{-10} \quad (2)$$

$$HONO + SF_6^- \rightarrow NO_2^-\cdot HF + SF_5 \qquad k_3 = 6.0 \times 10^{-10} \quad (3)$$

$$N_2O_5 + SF_6^- \rightarrow NO_3^- + SF_6 + NO_2 \qquad k_4 = 7.5 \times 10^{-10} \quad (4)$$

N_2O_5 was also detected in some experiments via its reaction with I^-,[28]

$$N_2O_5 + I^- \rightarrow NO_3^- + I \qquad k_5 = 2.0 \times 10^{-9} \qquad (5)$$

This second method was used because a small fraction of the reaction of SF_6^- with HNO_3 (~2%) yielded NO_3^- and interferred with N_2O_5 detection in the presence of HNO_3.[28] It should be noted that HNO_3, NO_2, or HONO do not react with I^-.

The uptake of HNO_3 was time-dependent; i.e., the decrease in HNO_3 signal after exposure to soot changed with time. The HNO_3 taken up by soot during exposure was released back to the gas phase when it was no longer exposed to HNO_3. Because the HNO_3 loss for a given exposure distance was not constant, one cannot calculate an uptake coefficient, γ, that is time independent. However, γ can be calculated from the corrected time-dependent first-order rate coefficient, k, at a given instant using the relation for a cylindrical reactor[30,31]

$$\gamma = 4kV/\omega S = 2rk/\omega \qquad (I)$$

where V is the volume of the flow tube, S is the geometric surface area of the soot coverage (55 cm^2), ω is the average molecular speed of HNO_3, and r is the radius of the flow-tube. Equation I is valid when diffusion is more rapid than loss at the wall. The measured first-order rate coefficient k was corrected for the radial concentration gradient generated by the uptake of HNO_3 onto soot surface using the method developed by Brown.[30] It is to be noted that even at the lowest temperature (where the uptake coefficients were much larger than that at 295 K), the maximum first-order loss rate coefficient of HNO_3, was ~200 s^{-1}, which was significantly lower than the diffusion-limited rate constant of 600 s^{-1} (i.e., the time-dependent uptake was not significantly limited by diffusion).

Fourier Transform Infrared Spectroscopy (FTIR). The infrared (IR) absorption studies involved measuring the spectrum of soot, in transmission mode, coated on a 25 mm diameter Ge disk that was placed inside an FTIR spectrometer (Figure 2). Spectra in the range between 450 and 4000 cm^{-1} were measured using this benchtop FTIR with a resolution of 1 cm^{-1}. The soot-coated Ge disk could be exposed to known concentration of HNO_3 for known periods of time. All these experiments were carried out at 295 K.

First, a polished Ge disk (i.e., without soot coating) was placed in the cell and a transmission spectrum, referred to as I_0, was measured. Then, this disk was removed and coated on one side with soot by burning TC-1 kerosene (aviation jet fuel) in a lantern in a manner similar to that used for coating the glass tubes and put back into the IR cell. The cell was pumped out and then exposed to various amounts of HNO_3 for known periods of time. After each exposure, the IR spectrum was recorded to obtain I. The ratios of I_0 to I yielded the spectra of the species on soot.

Materials and Sample Handling. HNO_3 was prepared by the reaction of concentrated H_2SO_4 with $NaNO_3$ followed by vacuum distillation of the mixture. HNO_3 was collected in a trap maintained at liquid N_2 temperature (77 K) and stored in a dry ice/2-propanol bath at 195 K. The concentrations of HNO_3 in the gas stream were measured by absorption at 184.9 nm (absorption cross section = 1.64×10^{-17} cm^2 $molecule^{-1}$) in a 50 cm long absorption cell before it was introduced into the NFT. The concentration of HNO_3 in the NFT was calculated from the He flow rate through HNO_3 reservoir, concentration of HNO_3 in the absorption cell, pressure and temperature in the absorption cell and in the NFT, and total flow rate through the NFT. The HNO_3 concentration was varied by varying the He flow rate over HNO_3 sample, the pressure in the HNO_3 reservoir and the bath temperature.

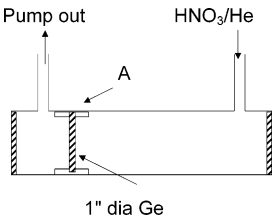

Figure 2. Schematic of the absorption cell inserted into the sample compartment of the FTIR spectrometer. A: Teflon cylindrical block which holds the 1 inch diameter Ge disc mounted inside the cell.

A mixture of 0.5% NO_2 in He was prepared manometrically in a darkened 12 L glass bulb for calibration of NO_2 CIMS signal. The concentration of HONO was determined from the relative rate constants of reactions 1 and 3.

Helium was used as the carrier gas in all the experiments and was flowed through electronic mass flow meters, which were calibrated by measuring the rate of change of pressure in a calibrated volume. For very high flow rates, a commercial calibrated water test meter was used in addition to a large calibrated volume.

Results and Discussions

Surface Area of Soot Samples. Specific surface areas of soot samples were determined with the single point BET method using N_2 as the adsorbate,[6] which is a modification of the procedure described by Nelsen and Eggertsen.[32] This method has been described previously[6] and is based on the adsorption of N_2 up to saturation by a sample at 77 K. The soot sample was exposed to N_2 from a gas stream of varying ratios of N_2 to He. The sample was warmed and the desorbed N_2 was measured by a thermal-conductivity detector. The amount of N_2 desorbed from the soot sample was compared with that from a reference soot sample of known surface area. Surface areas of soot samples produced under conditions identical to those used in uptake determination were measured. The *n*-hexane soot had a surface area of ~80 m^2 g^{-1}. Aviation kerosene, TC-1, soot had a surface area of ~100 m^2 g^{-1} (two samples: one with 105 and another with 97 m^2 g^{-1}). The surface area of one sample of TC-1 soot exposed many times to HNO_3 (to carry out the uptake experiments described earlier) was measured; it was 170 m^2 g^{-1}. On the basis of this limited data, we believe that the exposure of soot samples to HNO_3 increased the surface area by no more than a factor of 2. The measured specific surface area for *n*-hexane soot is roughly a factor of ~2 higher than the literature values and that for TC-1 soot is comparable to the specific surface area for kerosene soot.[14,33]

Uptake of HNO_3 Acid. The results of the measurements of HNO_3 uptake on soot samples generated from *n*-hexane and TC-1 are presented below.

Hexane Soot. Figure 3 shows the concentration of HNO_3 in the gas phase flowing out of the NFT as a function of time for which 13 mg of hexane soot was used. Initially, 1.7×10^{11} molecule cm^{-3} of HNO_3 in the gas phase was flowed through the injector but the injector was positioned beyond the soot-coated cylinder position marked B in Figure 1. The HNO_3 signal was constant. At time X, marked in Figure 3, the injector was withdrawn to position A in Figure 1 to expose the soot to HNO_3. There was an immediate decrease in HNO_3 signal, indicating removal of HNO_3 by soot. As time progressed, with the injector fixed at position A, the HNO_3 signal increased and eventually reached the value seen before exposure to soot. At time Y, the injector was moved back to a position B in Figure 1 where soot was not exposed to HNO_3 and HNO_3 signal increased instan-

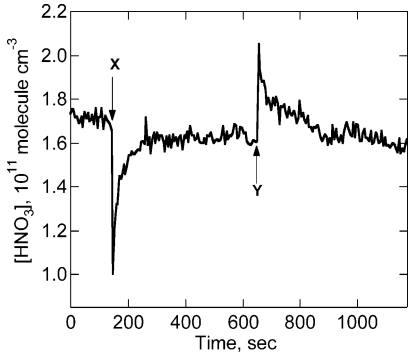

Figure 3. Time-dependent adsorption−desorption profile of HNO_3 uptake on 13 mg of *n*-hexane soot at 295 K. Time X and Y correspond to positions A and B respectively in Figure 1.

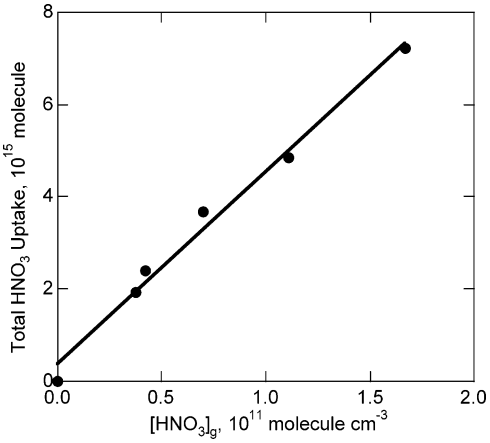

Figure 4. Total amount of HNO_3 adsorbed on 13 mg of hexane soot as a function of $[HNO_3]_g$ at 295 K.

taneously due to HNO_3 desorption from soot. The HNO_3 signal decreased as desorption continued and eventually reached the initial value equal to that where only the HNO_3 from the injector was present. The total HNO_3 taken up by soot was determined by integrating the time-dependent profile of HNO_3 concentration, shown in Figure 3, and using the flow velocity and the cross-sectional area of the flow tube to obtain the amount of HNO_3 molecules adsorbed on the soot surface. Desorption profiles were also similarly integrated to determine the amount of desorbed HNO_3.

Figure 3 indicates that HNO_3 uptake on soot is at least partially reversible. Further, quantitative analysis of the signal showed that the amount of HNO_3 adsorbed was nearly equal to the amount desorbed (>90%). This was true for all $[HNO_3]_g$ used in this study ($(4-17) \times 10^{11}$ molecule cm^{-3}). The amount of HNO_3 taken up by soot, as measured by either the loss from the gas phase upon exposure or increase in the gas phase upon desorption varied with the gas-phase HNO_3 concentration. Figure 4 shows a plot of the amount of HNO_3 adsorbed on the soot surface as a function of $[HNO_3]_g$ at 295 K. There is a linear increase in the amount taken up with partial pressure of HNO_3 (for $[HNO_3]_g < 2 \times 10^{11}$ molecule cm^{-3}) that appears to follow a Langmuir adsorption isotherm at low coverage.

At higher partial pressures of HNO_3, the uptake did not increase linearly with gas-phase concentration of HNO_3. But in all cases, all the HNO_3 desorbed from the soot, suggesting that the uptake of HNO_3 on soot was a reversible and nonreactive process. In addition to monitoring HNO_3 adsorption/desorption, we attempted to detect possible gas-phase products produced as soot was exposed to HNO_3. There was no detectable production of NO_2 or HONO as a result of the HNO_3 uptake.

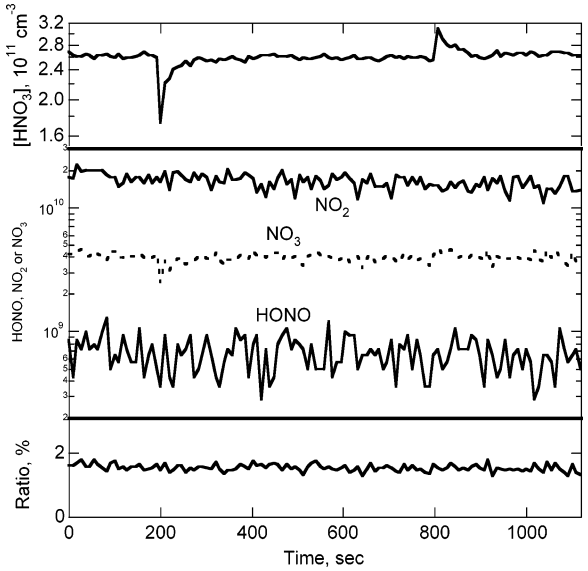

Figure 5. Upper panel: plot of $[HNO_3]_g$ against time as *n*-hexane soot (~13 mg) at 295 K was exposed to HNO_3 with the pressure in NFT = 3 Torr. Middle panel: concentrations of possible products HONO, NO_2, or NO_3 versus time as the same soot was exposed to HNO_3. Bottom panel: ratio of NO_3^- to $NO_3^-\cdot HF$ with exposure time. The NO_3^- ion could originate from the interaction of SF_6^- with NO_3, N_2O_5 or HNO_3. The featureless line of the ratio suggests that the sources of NO_3^- and $NO_3^-\cdot HF$ ions were the same; i.e., HNO_3 reacted with SF_6^- to generate both $NO_3^-\cdot HF$ and NO_3^-.

Figure 5 shows the plot of HNO_3 concentrations flowing out of the NFT for one adsorption−desorption cycle, $[HNO_3]_g = 2.6 \times 10^{11}$ molecule cm^{-3} at 295 K. The concentrations of possible product NO_2, HONO, N_2O_5 or NO_3 as a function of time are also displayed in the Figure 5 (see middle panel). The upper panel in Figure 5 shows the decrease in HNO_3 when exposed to soot. There were always detectable signals due to NO_2 and HONO (middle panel). However, their levels did not change upon exposure of HNO_3 to soot. The instantaneous loss of HNO_3 was as much as 1×10^{11} molecule cm^{-3} with changes in NO_2 being less than 5×10^9 (<5% of HNO_3 instantaneous loss) and changes in HONO being less than 1×10^9 molecule cm^{-3} (<1% of instantaneous loss of HNO_3).

The middle panel of Figure 5 shows the NO_3^- ion signal at $m/e = 62$. We attribute the ion signal at $m/e = 62$ to NO_3^- that is a minor product from the $SF_6^- + HNO_3$ reaction. The ratios of signals at $m/e = 62$ to those at $m/e = 82$ ($NO_3^-\cdot HF$) are plotted in the bottom panel. There was no clear temporal change in the signal, especially in congruence with exposure of HNO_3 to soot, which suggested that both signals at $m/e = 62$ and 82 originated from HNO_3. The measured ratio of NO_3^- to $HNO_3\cdot F^-$ signal yield a rate coefficient for the reaction

$$SF_6^- + HNO_3 \rightarrow NO_3^- + \text{product} \qquad (1b)$$

of $\sim 4 \times 10^{-11}$ cm^3 $molecule^{-1}$ s^{-1} assuming no mass discrimination between NO_3^- and $NO_3^-\cdot HF$ by mass filter and channeltron. If either N_2O_5 or NO_3 was produced, they would have been taken up by soot reactively and the ratio of the two signals would have changed during adsorption−desorption cycle.[16] Further, N_2O_5 or NO_3 would have reacted with soot to produce NO_2 and we should have seen a change in NO_2 signal (middle panel). The absence of NO_2 production also suggests that the extent of conversion of HNO_3 to NO_2 is small (<5% of HNO_3 adsorbed).

In these experiments, 13 mg of hexane soot with a surface area of $\sim 1 \times 10^4$ cm^2 (~80 m^2 g^{-1}) was used. The uptake of

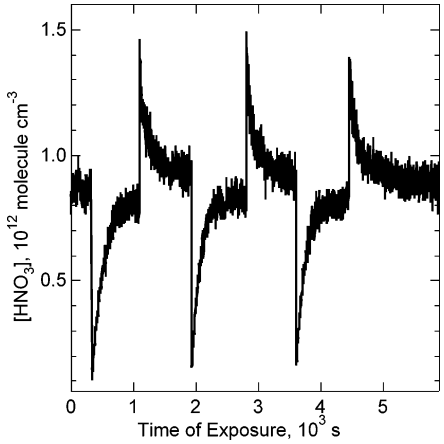

Figure 6. Time-dependent profile of $[HNO_3]$ exiting the TC-1 soot-coated flow tube as the soot sample (60 mg TC-1 soot) was subjected to adsorption−desorption cycles at 295 K (see text for description of the cycles). $[HNO_3]$ at the entrance of the flow tube was 8.9×10^{11} molecule cm^{-3}.

TABLE 1: Total Number of HNO_3 Molecules Taken up and Desorbed in Different Adsorption−Desorption Cycles[a]

	total no. of molecules, 10^{17}		
adsorption−desorption cycle	adsorption	desorption	desorption/ adsorption ratio
1	3.12	2.77	0.89
2	2.93	2.46	0.84
3	2.67	2.74	1.03
4	2.70	2.68	0.99

[a] 60 mg TC-1 soot, temperature = 295 K, pressure = 3.2 Torr in He, flow velocity = 992 cm s^{-1}, $[HNO_3]_g = 8.9 \times 10^{11}$ molecule cm^{-3}.

HNO_3 was 7×10^{15} molecules at $[HNO_3]_g$ of 1.7×10^{11} molecule cm^{-3} at 295 K or 6.9×10^{11} molecules cm^{-2} on the basis of the surface area being determined via the method described earlier. This roughly represents 0.3% of a monolayer coverage, which is $\sim 6 \times 10^{14}$ molecule cm^{-2}.[14] (The molecular area of HNO_3 is estimated from the Lennard-Jones parameter ($\sigma_{LJ} = 3.91$ Å)[34] to be ~16 $Å^2$ $molecule^{-1}$ or $\sim 6 \times 10^{14}$ molecule cm^{-2} for a monolayer.)

The low coverage is consistent with the observation of Aubin and Abbatt[14] at low $[HNO_3]_g$, where they measured an uptake of $\sim 6 \times 10^{11}$ molecule cm^{-2} for a $[HNO_3]_g$ of $\sim 1.6 \times 10^{11}$ molecules cm^{-3} at 295 K (Figure 6 of Aubin and Abbatt[14]). We did not investigate the behavior of HNO_3 at high concentration or as a function of temperature because Aubin and Abbatt have already reported nonlinear adsorption at high HNO_3 concentration.

TC-1 Soot. In contrast to the limited works on *n*-hexane soot, TC-1 soot was studied more extensively, using two different samples (5.7 mg and 60 mg), a large range of gas-phase HNO_3 concentrations, $[HNO_3]_g$ (varied in the range: $6-670 \times 10^{10}$ molecule cm^{-3}), and three different temperatures (253, 273 and 295 K). Both soot samples (5.7 and 60 mg) behaved identically and we describe in detail only the results from the 60 mg sample.

The time-dependent signal due to HNO_3 with $[HNO_3]_g = 8.9 \times 10^{11}$ molecule cm^{-3} exposed to a 60 mg sample of TC-1 kerosene soot at 295 K is shown in Figure 6. The uptake and desorption of HNO_3 was studied on TC-1 kerosene soot using methodologies identical to those employed for *n*-hexane soot. Fresh soot was subjected to successive adsorption/ desorption cycles. In the first cycle (see Table 1) there was a net loss of HNO_3 to the soot. Whereas in the following cycles net desorption was equivalent to net adsorption. This observation suggests that the effective surface area available for the first exposure to soot ("unexposed") was larger than those for the three subsequent cycles. In other words, a small measurable fraction of HNO_3 taken up by TC-1 soot was not released to the gas phase at 295 K.

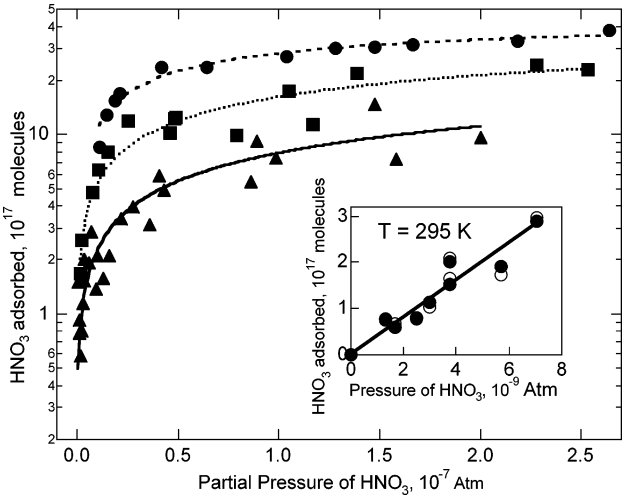

Figure 7. Amount of HNO_3 adsorbed on 60 mg of TC-1 soot as a function of equilibrium partial pressures of HNO_3 at three different temperatures: (▲) 295 K; (■) 273 K; (●) 253 K. Solid and dotted curves are fits of the data to Langmuir−Freundlich form (see text for details, eq IV). Inset: isotherm with expanded scale of $P(HNO_3)$ at low partial pressures (adsorption (●); desorption (○)) are shown.

In the case of TC-1 soot, the amount of HNO_3 taken up increased with increasing $[HNO_3]_g$ and increased with decreasing temperature. In experiments carried out at 253 and 273 K, the amount of HNO_3 taken up was always greater than that desorbed from the soot by a factor of approximately 2 at the same temperature in the first two adsorption−desorption cycles. After each adsorption/desorption experiment, we determined the amount of HNO_3 left on the surface by integrating the time-dependent adsorption−desorption profiles. The amount of HNO_3 taken up by soot in equilibrium with HNO_3 as a function of time in the flow tube during the adsorption period was determined. Desorbed HNO_3 from the surface was also measured and desorption profiles were integrated to determine the amount of desorbed HNO_3. Then, the HNO_3 flow was turned off and the flow tube was heated to 373 K to completely remove HNO_3 from soot. The total amount of HNO_3 taken up by soot was roughly equal (within 5−10%) to the HNO_3 desorbed at the same temperature as the adsorption plus that evolved during the temperature programmed desorption up to 373 K.

Adsorption Isotherm. Figure 7 shows the total number of molecules of HNO_3 adsorbed on the 60 mg TC-1 soot sample as a function of the gas-phase partial pressure of HNO_3 at three different temperatures. These uptake values were determined from the first adsorption profile (i.e., carried out on "fresh" soot, for which all HNO_3 had been removed by heating it to 373 K). At the highest values of $[HNO_3]_g$ (7×10^{12} molecule cm^{-3}) and at the lowest temperature (253 K) employed in our studies, the coverage was ~12% of a monolayer (assuming a monolayer coverage of 6×10^{14} molecule cm^{-2}). At low $[HNO_3]_g$ ($<2.5 \times 10^{11}$ molecule cm^{-3} or $<10^{-8}$ atm), the coverage on soot increased linearly with $[HNO_3]_g$, i.e., behaved in a manner consistent with a Langmuir isotherm (see inset in Figure 6). As $[HNO_3]_g$ increased, the uptake process showed deviation from the Langmuir behavior. Non-Langmuir behavior can arise from (1) the heterogeneity of the surface such that different sites have

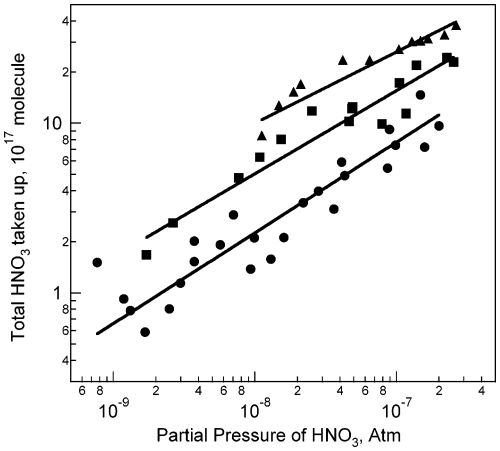

Figure 8. HNO_3 adsorbed (on a log scale) versus equilibrium partial pressures of HNO_3 (on a log scale): (●) $T = 295$ K, $\nu_1 = 0.53 \pm 0.12$; (■) $T = 273$ K, $\nu_1 = 0.49 \pm 0.17$; (▲) $T = 253$ K, $\nu_1 = 0.42 \pm 0.18$. The solid lines are fits of the data to Freundlich isotherms (eq III).

different binding energies (i.e., differing heats of adsorption or adsorption energies), (2) a HNO_3 molecule occupying more than one site, or (3) HNO_3 molecules undergoing dissociation. This kind of behavior is common for a substrate with nonuniform sites, as is likely the case for soot. The adsorption data for a nonuniform surface can be fit to a Freundlich isotherm,[35]

$$\frac{\theta}{\theta_m} = AP^{\nu_1} \qquad \text{(II)}$$

where θ is the total number of adsorbed molecules of HNO_3, θ_m is the total number of HNO_3 molecules for a monolayer coverage, P is the partial pressure of HNO_3 in atmospheres, A is a constant and ν_1 is the heterogeneity parameter. This form assumes that the adsorption energy distribution function is exponential in θ/θ_m.

The linearized form of eq II can be written as

$$\log \theta = \log A + \nu_1 \log P + \log \theta_m \qquad \text{(III)}$$

The plots of θ (on a log scale) versus partial pressure of HNO_3, $P(HNO_3)$ (on a log scale) are shown in Figure 8 for temperatures 253, 273 and 295 K. The slopes (ν_1) of the plots are 0.42 ± 0.18, 0.49 ± 0.17 and 0.53 ± 0.12 for 253, 273 and 295 K, respectively. The errors are 2σ precision in the slope obtained by linear least-squares analysis. The values of ν_1 are nearly equal to 0.5 in the temperature range 273−295 K, which suggests that a HNO_3 molecule is adsorbed on two different sites and/or the surface is heterogeneous.[14] Alternatively, our data can be fit to Langmuir−Freundlich (L−F) isotherm of the form

$$\frac{\theta}{\theta_m} = \frac{(K_{eq}P)^{\nu_2}}{1 + (K_{eq}P)^{\nu_2}} \qquad \text{(IV)}$$

where K_{eq} is the equilibrium constant for partitioning between the gas phase and the soot surface and ν_2 is the heterogeneity parameter to compensate for a nonuniform surface and/or dissociative adsorption (i.e., dissociation of a HNO_3 molecule on the surface to occupy two sites or adsorption of a HNO_3 molecule occupying two sites without undergoing dissociation). θ, θ_m and P are as defined earlier. The fit of data in Figure 7 to eq IV yielded K_{eq}, θ_m and ν_2 at three different temperatures. These parameters are listed in Table 2a. This was the form of isotherm used by Aubin and Abbatt.[14] Equation IV is a

TABLE 2: Equilibrium Constant (K_{eq}) and Monolayer Coverage (θ_m) for 60 mg of TC-1 Soot

(a) Heterogeneity Parameter Calculated from Eq IV

temp (K)	K_{eq} (atm^{-1})	θ_m (10^{18} molecule)	ν_2
295	7.6×10^5	4.5	0.6 ± 0.2
273	3.51×10^6	4.8	0.6 ± 0.2
253	1.62×10^7	4.8	0.7 ± 0.25

(b) Heterogeneity Parameter Fixed to 0.5

temp (K)	K_{eq} (atm^{-1})	θ_m (10^{18} molecule)	ν_2
295	2.69×10^4	15.6	0.5
273	2.97×10^5	10.8	0.5
253	4.14×10^6	7.1	0.5

convenient way to parametrize the isotherm data. However, the interpretation of the equilibrium constant, K_{eq}, derived from this fit depends on the mechanism of adsorption. Because, for a nonuniform surface like soot, the heat of adsorption can change with coverage, the equilibrium constant, K_{eq}, derived from fits to eq IV represents an average value over the range of coverages. Similarly, the heat of adsorption, $\Delta^0 H_{ads}^{van't Hoff}$, derived from a van't Hoff analysis (plot of ln K_{eq} vs $1/T$, shown in Figure 9),

$$\ln K_{eq} = -\frac{\Delta^0 H_{ads}^{van't Hoff}}{T} + \text{constant} \qquad \text{(V)}$$

would also be an average value over the entire coverage. The K_{eq} values (Table 2a) were converted to unitless equilibrium constant appropriate for the surface using the standard state defined by Kemball and Rideal[36,37] and used by Aubin and Abbatt.[14] The conversions were done as follows. The standard state for a surface was taken to be $\sim 1.6 \times 10^{12}$ molecule cm^{-2},[34] which is the coverage when molecules are distributed similarly to that in the gas phase at the standard state. The unitless equilibrium constant, K_{uleq}, is defined as the ratio of the measured surface concentration at a given $[HNO_3]_g$ to the surface concentration at standard state and is given by $K_{uleq} = K_{eq}\ (6 \times 10^{14}/1.6 \times 10^{12})$.[14] These values are shown in Table 3a. The slope of the plot of ln(K_{eq}) against $1/T$ (see Figure 8) yields $\Delta^0 H_{ads}^{van't Hoff} = -10.8 \pm 2.1$ kcal mol^{-1}. It should be noted that the $\Delta^0 H_{ads}^{van't Hoff}$ value, which arises as a slope of ln(K_{eq}) vs $1/T$ plot, is not changed by the above unit conversion.

If dissociative adsorption is taking place, ν_2 should be equal to 0.5.[14] Our average ν_2 value at three temperatures 295, 273 and 253 K was 0.63 ± 0.25 and it is therefore possible that a

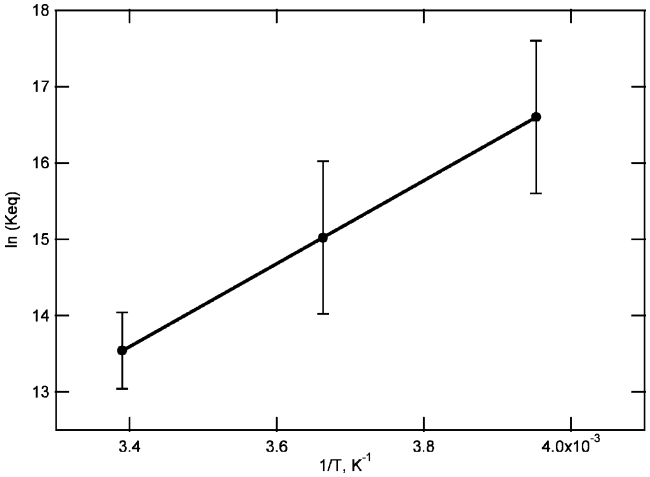

Figure 9. ln(K_{eq}) versus $1/T$. K_{eq} values were obtained by fitting the adsorption isotherm data to a Langmuir−Freundlich form (eq IV in text). The line is a fit of the data to a van't Hoff equation (eq V).

TABLE 3: Unitless K_{eq} and Free Energy of Adsorption Determined for 60 mg of TC-1 Soot

(a)

temp (K)	K_{eq} (atm^{-1})	K_{uleq} (unitless)	Δ^0H (van't Hoff fit) (kcal mol^{-1})	estimated Δ^0S[a] (cal mol^{-1} K^{-1})	$\Delta^0G = -RT\ln(K_{eq})$ (kcal mol^{-1})	$\Delta^0H = \Delta^0G - T\Delta^0S$
295	7.6×10^5	2.9×10^8	-10.8 ± 2.1	-17.6	-11.4	$-(16.6 \pm 2.1)$
273	3.5×10^6	1.3×10^9		-19.8	-11.3	$-(16.7 \pm 2.1)$
253	1.6×10^7	6.1×10^9		-22.3	-11.3	$-(17.0 \pm 2.1)$

(b) K_{eq} Values from Table 2b for $\nu_2 = 0.5$

temp (K)	K_{eq} (atm^{-1})	K_{eq} (unitless)	Δ^0H (van't Hoff fit) (kcal mol^{-1})	estimated Δ^0S[a] (cal mol^{-1} K^{-1})	$\Delta^0G = -RT\ln(K_{eq})$ (kcal mol^{-1})	$\Delta^0S = (\Delta^0H - \Delta^0G)/T$
295	2.69×10^4	1.0×10^7	-17.5 ± 1.0	-17.6	-9.4	-27.5
273	2.97×10^5	1.1×10^8	-17.3 ± 3.5 (50% error)	-19.8	-10.0	-27.5
253	4.14×10^6	1.6×10^9	-17.5 ± 5.0 (100% error)	-22.3	-10.6	-27.3

[a] Entropies of adsorption were calculated using statistical thermodynamics.[35]

dissociative adsorption process occurs on TC-1 soot. The absence of detectable NO_2, one of the likely dissociation products, during desorption from the soot surface suggests, but does not exclude, the absence of the dissociative adsorption process (i.e., desorption can occur via recombination), suggesting that a multiple interpretation is plausible.

The derived monolayer coverages, θ_m, at three temperatures, shown in Table 2a, are in excellent agreement (within 10%) with each other. The BET surface area of our 60 mg sample of soot was 6×10^4 cm^2 ($\sim$100 m^2 g^{-1}). Taking the occupied area by each HNO_3 molecule as $\sim 1.6 \times 10^{-15}$ cm^2 $molecule^{-1}$, we calculate that $\sim 3.8 \times 10^{19}$ molecule would be equivalent to a monolayer coverage on our soot sample. The experimentally determined values of θ_m (4.5×10^{18}) are $\sim$12% of the value determined from the BET surface area measured using N_2 and if we assume that each molecule is adsorbed at one site. However, it is possible that not all sites that are available to N_2 are available to HNO_3 because of porosity, nonuniformity, etc. of the soot.

If we fix ν_2 to be 0.5 (see Table 2b), the parameters obtained by fitting our isotherm data to eq IV yield θ_m that is 2$-$4 times higher and the heat of adsorption, $\Delta^0H_{ads}^{van'tHoff}$, is -17.3 ± 3.5 kcal mol^{-1} (see Table 3b). The higher values of θ_m are closer to the BET surface area measured with N_2.

In the above analysis, interpretation of K_{eq}, $\Delta^0H_{ads}^{van'tHoff}$ and ν_2 depends on our interpretation of the adsorption mechanism. This difficulty can be bypassed by calculating the isosteric heats of adsorption, which do not depend on the specific mechanism but are of practical use. The isosteric heats of adsorption, $\Delta^0H_{ads}^{isosteric}$, are defined below.

$$\ln(P_{eq}) = -\frac{\Delta^0H_{ads}^{isosteric}}{T} + \text{constant} \qquad \text{(VI)}$$

The $\Delta^0H_{ads}^{isosteric}$ values calculated for isosteric conditions would be dependent on the coverage. The partial pressures (P_{eq}) of HNO_3 in equilibrium with a specified coverage are calculated for different temperatures using Langmuir$-$Freundlich isotherm expression (eq IV). The plots of $\ln(P_{eq})$ versus $1/T$ are shown in Figure 10 for 3 different coverages. The slopes of these plots yield $\Delta^0H_{ads}^{isosteric}$, which are clearly dependent on the coverage. The heats of adsorption were determined to be -15.3 ± 1.0, -14.1 ± 0.5 and -13.4 ± 0.5 kcal mol^{-1} for 1.6%, 3.2% and 4.8% coverage, respectively, and decrease systematically with increasing coverage, which is reasonable. A linear extrapolation of these data to zero coverage yields a value of ~ -16 kcal mol^{-1}. It is not clear if such an extrapolation is valid.

Gas-Phase Products. To ascertain if HNO_3 uptake leads to discernible products, NO_3, N_2O_5, HONO, and NO_2 were also monitored when HNO_3 was exposed to soot. There was no N_2O_5 detected as an impurity in the HNO_3 sample. SF_6^- was used as the reagent ion to simultaneously detect all the above species including HNO_3. Figure 11 shows a plot of HNO_3 adsorption$-$desorption profile at 238 K along with signals for HONO and NO_2. There was no measurable production of NO_2 or HONO. In a separate study on the uptake of N_2O_5 on TC-1 soot it was shown that $\sim$65% of N_2O_5 taken up was converted to NO_2.[38] Therefore, we believe that if N_2O_5 were produced, we would have seen the production of NO_2. However, we did not observe any NO_2 production as a result of HNO_3 uptake on soot. On the basis of the detection sensitivity for NO_2, the upper limit for N_2O_5 production from HNO_3 uptake was deduced to be less than 0.1%. Figure 11 (middle panel) also shows the time-dependent NO_3^- signals at $m/e = 62$ when soot was exposed to HNO_3. The ratio of signal at $m/e = 62$ (see middle panel) to the ion signal at $m/e = 82$ (top panel) is plotted in the bottom panel. The time-dependent profiles were identical to those for hexane soot. Using the same arguments as in the case of hexane soot, we conclude that HNO_3 uptake on TC-1 soot did not produce any NO_3 or N_2O_5. The above experiments demonstrate that HNO_3 uptake on TC-1 soot does not produce significant amounts of NO_2, HONO, NO_3 or N_2O_5.

Comparison between Hexane and TC-1 Soot. Exposure of HNO_3 to both *n*-hexane and TC-1 soot did not produce any measurable products. Therefore, we conclude that HNO_3 is reversibly taken up by both types of soot and no chemically distinguishable products are generated. As described earlier, the HNO_3 coverage was 0.1% of the BET surface area of *n*-hexane soot for a $[HNO_3]_g$ of 1.7×10^{11} molecules cm^{-3}. In contrast, for TC-1 soot, the coverage was $\sim$0.8% of the BET surface area for a similar value of $[HNO_3]_g$ (1.74×10^{11} molecules

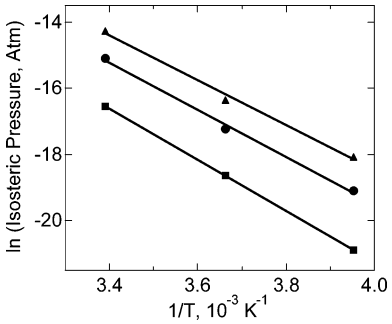

Figure 10. Plots of ln(Isosteric equilibrium partial pressure of HNO_3) versus $1/T$: (■) coverage $= 5 \times 10^{17}$ ($\sim$1.6%), $\Delta^0H_{ads}^{isosteric} = -(15.3 \pm 0.2)$ kcal mol^{-1}; (●) coverage $= 1 \times 10^{18}$ ($\sim$3.2%), $\Delta^0H = -(14.1 \pm 0.5)$ kcal mol^{-1}; (▲) coverage $= 1.5 \times 10^{18}$ ($\sim$4.8%), $\Delta^0H = -(13.4 \pm 0.5)$ kcal mol^{-1}. The lines are fit to the isosteric free energy relationship (eq VI).

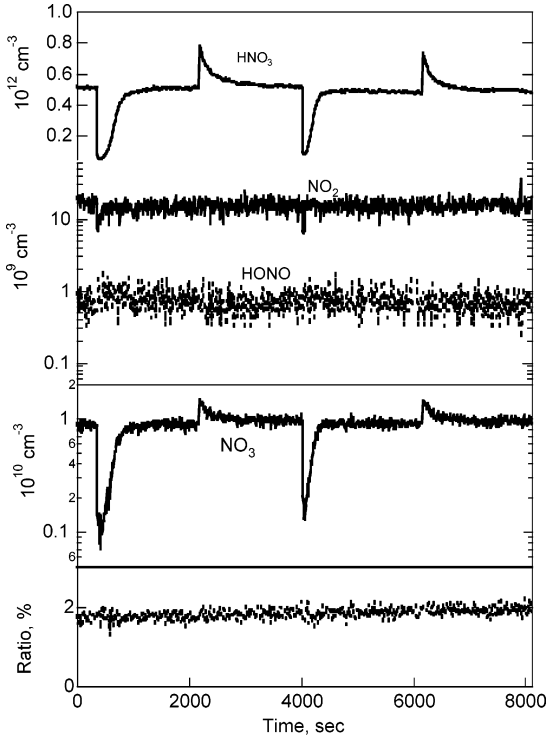

Figure 11. Upper panel: (top trace) time-dependent concentration profile of HNO_3; (lower traces) concentrations of possible products, HONO and NO_2, as a function of time as the TC-1 soot sample was exposed to HNO_3 at 238 K. Middle panel: NO_3^- signal at mass 62, which could come from NO_3, N_2O_5 or HNO_3. Bottom panel: NO_3^- signal as percent of HNO_3 signal. Type of soot: 5.7 mg of TC-1 soot.

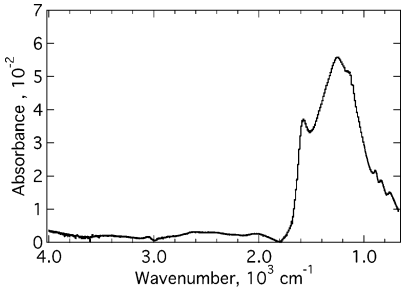

Figure 12. FTIR Spectrum of TC-1 kerosene soot.

cm^{-3}). Thus the uptake of HNO_3 on TC-1 soot was ~8 times greater than that on hexane soot per unit BET surface area of the soot sample at 295 K. It should be noted that uptake per unit BET surface area depends only on the equilibrium gas-phase concentration of HNO_3, heat of adsorption and temperature.

Last, identical results were obtained for the 5.7 mg TC-1 soot sample. Therefore, it is clear that our results were not sensitive to the soot amount or soot preparation.

FTIR Studies. Figure 12 shows the infrared spectrum of a TC-1 soot sample deposited on a Ge disk. This spectrum shows the presence of organic functional groups such as aromatic carbonyl (−C═O) groups at 1583 cm^{-1}, −C−C−, −C═C− (C−C single bonds and double bonds),[19] and aromatic substrates (600−900 cm^{-1}). This soot was exposed to ~2.5×10^{12} molecule cm^{-3} (8×10^{-5} Torr) of HNO_3 at 295 K and at a total pressure of ~12 Torr of He for up to 30 min. The absorption spectra were monitored every 10 min. The exposure time was comparable to that in the previously described uptake experiments at 295 K. On the basis of the HNO_3 uptake measured in the flow tube, roughly 1×10^{14} molecule cm^{-2} (geometrical surface area) of HNO_3 should have been left on the soot surface. Yet no measurable changes in the IR spectrum were detected. (At these vapor pressures of HNO_3, there was no detectable gas-phase absorption due to HNO_3, as demonstrated by a separate experiment). Organic nitrate or nitro compound, if produced in sufficient quantities, should have been clearly seen. In contrast, when we flowed N_2O_5 ($[N_2O_5] = 2 \times 10^{12}$ molecule cm^{-3} at a flow rate of 30 sccm of He for 2 min) over the same soot sample the absorption features of organic nitrates appeared (asymmetric stretching of $-NO_2$ group at 1585−1650 cm^{-1}, symmetric stretching of $-NO_2$ group at 1220−1320 cm^{-1}, $-NO_2$ bending at 700−730 cm^{-1} and stretching of π-bonds of N−O linkage at 800−930 cm^{-1}) within a few minutes of onset of exposure.[38] On the basis of the detection sensitivity, we conclude that less than 1% of adsorbed HNO_3 perhaps reacted to make any solid-phase products. Thus we believe there was no other product formed on the soot surface as a result of the interaction of HNO_3 with soot.

Comparison with Previous Studies. *Chemical Reactivity.* In our experiments, the uptake of HNO_3 on hexane and aviation kerosene (TC-1) soot was reversible (with $P(HNO_3) \leq 2 \times 10^{-4}$ Torr) and did not produce measurable amount of HONO, NO_2, NO_3 or N_2O_5 in the temperature range 295−253 K. We compare our results with those from previous studies in Table 4. The table lists the type of soot, the partial pressures of HNO_3 and the products that were detected. In a previous study from this laboratory, Longfellow et al.[16] reported negligible conversion of HNO_3 to NO_2 (<3%) and NO (10%) on kerosene soot and methane soot at 296 K. However, they did not attempt to measure the production of N_2O_5/NO_3 or HONO. Kleffman and Wiesen,[15] Aubin and Abbatt,[14] and Saathoff et al.,[39] also did not observe any significant formation of NO_2 as described below. Kleffman and Wiesen[15] reported that NO and HONO were unobservable when soot was exposed to 600 ppbv ($P(HNO_3)$) = 4.6×10^{-4} Torr) of HNO_3 for 2 days. However, at higher partial pressures of HNO_3, $P(HNO_3) > 800$ ppbv (6.1×10^{-4} Torr), NO and NO_2, but not HONO, were detected. Aubin and Abbatt[14] also reported reversible (within 20%) uptake of HNO_3 between 228 and 295 K. They could not detect the formation of NO_2, HONO and NO because of interference from HNO_3 in their experimental method. Again, as in the case of Kleffman and Wiesen[15] at high partial pressures of HNO_3 ($0.6-6 \times 10^{-4}$ Torr) Aubin and Abbatt[14] did observe a steady loss of HNO_3. Choi and Leu[33] studied the HNO_3 uptake on Degussa F2 (an amorphous black carbon), graphite, *n*-hexane soot and kerosene soot. They did not detect any measurable decomposition of HNO_3 on flame deposited *n*-hexane and kerosene soot up to partial pressure of HNO_3, $P(HNO_3) = 5 \times 10^{-4}$ Torr (1.62×10^{13} molecule cm^{-3}). The uptake was reversible at 295 K and irreversible at 220 K. Significant HNO_3 decomposition was observed on FW2 soot at 295 K with $P(HNO_3) \geq 1 \times 10^{-4}$ Torr but no decomposition was observed at 220 K. Similar decomposition was observed on graphite soot but was much smaller compared to that on FW2 soot. When HNO_3 partial pressures in all these experiments were low, closer to atmospheric conditions, there was no significant conversion of HNO_3.

Kirchner et al.[19] observed slow or steady-state uptake of HNO_3 on GfG soot (spark generated graphite soot) with γ in the range 1×10^{-7} to 2×10^{-6} (assuming BET surface area). The partial pressures of HNO_3 were fairly high (up to 6.8 mTorr). FTIR spectra of the soot after reaction with HNO_3 revealed bands attributable to organic nitrates, $R-O-NO_2$ (1660, 1280 and 825 cm^{-1}) and nitro compounds, $R-NO_2$ (1565

TABLE 4: Comparisons of HNO_3 Uptake on Soot

investigator	soot type/surface area ($m^2\ g^{-1}$)	HNO_3 partial pressure (atm)/T (K)	comments	uptake coefficients (eq I)
Choi and Leu[33] flow tube/QMS	hexane soot/46	$(0.41-5.3) \times 10^{-7}$/295	no detectable product formation; followed Langmuir up to 2×10^{-7} atm; uptake is time-dependent and reversible	0.023 ± 0.004 at 295 K[a]
	Degussa FW2/368	6.6×10^{-10}/294 and 220	reversible and no product at 294 K; irreversible at 220 K and adsorbed HNO_3 decomposes on desorption at 353 K and produces NO_2, NO, CO_2, H_2O and some unidentified volatile products	0.067 ± 0.005 at 295 K[a] 0.13 ± 0.01 at 220 K[a]
	graphite soot/15	6.6×10^{-10}/294 and 220	behaves simlar to Degussa FW2 soot	
	Degussa FW2/368	$(1.3-5.7) \times 10^{-7}$/295	HNO_3 decomposes to make NO_2	
		$(1.3-5.7) \times 10^{-7}$/220	no decomposition of HNO_3	
	kerosene soot/91	8×10^{-10} to 2.8×10^{-7}	no decomposition at 295 K, but at 219 K, the uptake is irreversible and HNO_3 seemed to decompose at 323 K during thermal desorption	0.060 ± 0.005 at 295 K[a] 0.093 ± 0.002 at 220 K[a]
Longfellow et al.[16]	kerosene soot/∼100	3.7×10^{-10}/296	uptake is reversible and time dependent; upper limits for NO_2 and NO production: <3% and <10% of HNO_3 uptake, respectively	5×10^{-5} [b]
	methane soot	3.7×10^{-10}/296	uptake is reversible and time dependent; upper limits for NO_2 and NO production: <3% and <10% of HNO_3 uptake	
Kleffmann and Wiessen[15]	Degussa Lamp Black/101 and 20	$<6 \times 10^{-7}$	uptake is reversible (within 90%); no production of NO_2, NO or HONO	
		$>8 \times 10^{-7}$	NO and NO_2 generated but no HONO	
Kirchner et al.[19]	GfG, spark generated graphite soot/200	$(2.2-90) \times 10^{-7}$	organic nitrate, nitrite and nitro compounds generated on the soot surface; no attempts were made to detect the gas-phase products	initial uptake: $(2.3-0.28) \times 10^{-4}$ longer term slow uptake: $(1.9-0.78) \times 10^{-6}$ [a]
Rogaski et al.[22]	Degussa lamp black FW2/460	$(6.6-130) \times 10^{-7}$/296	66% of adsorbed HNO_3 converted to NO and NO_2 and H_2O	0.038[a]
Prince et al.[21]	Degussa lamp black FW2/460	$(66-330) \times 10^{-7}$/296	33% of lost HNO_3 converted to NO_2	4×10^{-7}[b]
Saathoff et al.[17]	spark generated graphite soot/200	5×10^{-7}	no significant formation of NO_2	upper limit: $\leq 3 \times 10^{-7}$ [b]
Disselkamp et al.[18]	Degussa FW2/460 crystalline graphite Cabot Monarch/1000	3×10^{-5}/298	each type of soots yielded similar chemistry; NO_2 production varied between 35 and 85% of HNO_3 lost	
Aubin and Abbatt[14]	hexane/30	$(3.3-800) \times 10^{-7}$/228−295	uptakes were mostly reversible (within 90%); no products were detected	steady-state uptake coefficient: 1.3×10^{-3} for 3.6×10^{-8} atm of HNO_3 [a]
Salgado Munoz and Rossi[20]	gray decane soot (fuel rich flame)/69	$(0.4-3.7) \times 10^{-7}$/295	produces mostly HONO with yield in the range 34−68%	
	black decane soot (lean fuel)	$(0.4-3.7) \times 10^{-7}$/295	uptake mostly reversible with NO yields of 7−23%	
this work	hexane soot/78	$(1.2-12) \times 10^{-9}$/295	reversible uptake; no product formation	
	TC-1 kerosene (aviation kerosene)/105	$(7-280) \times 10^{-10}$/253−295	uptakes were reversible; no gas-phase products were detected; no solid-phase products were detected on the surface of the soot	

[a] Based on geometrical surface area. [b] On the basis of BET surface area.

and 1320 cm^{-1}). They did not specify the extent of product formation. This contrasts with the lack of products observed in the present study in the FTIR and in the flow tube at low concentrations of HNO_3. Rogaski et al.[22] used very high partial pressures, 0.5−10 mTorr, of HNO_3 and observed $\gamma = 0.038$ for the loss of HNO_3 and determined that 66% of adsorbed HNO_3 was converted to NO and NO_2 on Degussa black carbon soot. Prince et al.[21] used 5−25 mTorr of HNO_3 ($(1.6-8) \times 10^{14}$ molecule cm^{-3}) and observed a long-term steady-state uptake coefficient for loss of HNO_3 on black carbon soot ($\gamma = 4 \times 10^{-7}$ for a BET surface area) to produce NO_2. They claimed that 33% of the loss of HNO_3 produced NO_2. In these studies, where reactive uptake of HNO_3 was observed with gas-phase product formation, concentrations of HNO_3 were high.

From all these studies, it appears that HNO_3 is not converted to other products (i.e., HNO_3 is not destroyed) on soot when the partial pressures of HNO_3 are small (5×10^{-4} Torr). However, at high partial pressures of HNO_3, it appears that there are reactions. One possibility is that at high partial pressures of HNO_3 there is a pathway for the formation of N_2O_5 (i.e., dehydration of HNO_3) and such a process is not feasible at low pressures of HNO_3. The study by Munoz and Rossi[20] contradicts the findings of other studies that used low partial pressures and reported no product formation. They used a reasonably low $[HNO_3]_g$ and exposed it to gray decane soot ($(1-9) \times 10^{12}$ molecule cm^{-3} or $P(HNO_3) = (3-27) \times 10^{-5}$ Torr) and on black decane soot ($(0.2-6) \times 10^{12}$ molecule cm^{-3}, $P(HNO_3) = (6-185) \times 10^{-6}$ Torr) and observed production of NO_2, HONO, and NO. They reported a $\gamma = 5 \times 10^{-4}$ to 2×10^{-2} (calculated using geometric surface area) on lamp soot and 34−68% of lost HNO_3 was converted to HONO. It is not clear why they observed such a high yield for conversion of HNO_3. The possibility that these soot samples were some how more reactive cannot be excluded.

Physical Uptake. Previous studies on different types of soot have indicated that HNO_3 is taken up reversibly. The mechanism of uptake and the energetics involved are unclear. The heterogeneity parameter, ν_2, we measured, ranges from 0.6 to 0.7 (Table 2a), similar to those determined by Aubin and Abbatt[14] (0.5 ± 0.07) on *n*-hexane soot. A value of ∼0.5 could arise from roughness of the soot surface, sites with different heats of adsorption, dissociative adsorption of HNO_3 molecule or uptake on two sites without undergoing dissociation. The average heat of adsorption (-10.8 ± 2.1 kcal mol^{-1}) we determined on TC-1 soot using a van't Hoff analysis is in reasonable agreement with that (-13.3 ± 1.8 kcal mol^{-1})) obtained on *n*-hexane soot by Aubin and Abbatt.[14]

For soot surfaces, the isosteric heats of adsorption are more representative than that obtained by analysis using eq IV, i.e., the Langmuir−Freundlich isotherm. Our isosteric heats of adsorption decrease with increasing coverage, which is reasonable. The reason for this decrease could be due to sites of different binding energy and/or interaction between adsorbed molecules. Our isosteric heats of adsorption for TC-1 soot are ∼20% higher than that reported by Aubin and Abbatt[14] for *n*-hexane soot, for a coverage that they did not specifically note in their paper.

Atmospheric Implications. We estimate below the amount of nitric acid taken up by atmospheric aerosols based on our results. The surface area of aerosols in a well processed urban air mass is $\sim(2-6) \times 10^{-6}$ cm^2 cm^{-3} (under 1 μm size particles) and the nitric acid abundance is ∼20−50 ppbV ($(5-12.5) \times 10^{11}$ molecule cm^{-3} at 1 atm). We assume a surface area density of 6×10^{-6} cm^2 cm^{-3}, a $P(HNO_3)$ of 50 ppbv ($\sim 1 \times 10^{12}$ molecule cm^{-3}) and a black carbon content (externally mixed) of ∼10%. Under these conditions, the surface coverage at 253 K (Figure 7) on black carbon (BC) would be $\sim 1 \times 10^{14}$ molecule cm^{-2} (20% coverage). Therefore, only 6×10^7 molecules cm^{-3} of nitric acid would be taken up by aerosol. This amount is negligible compared to the gas-phase concentration of $\sim 1 \times 10^{12}$ molecule cm^{-3}. Even if the isosteric heat of adsorption was much larger, we estimate the uptake of HNO_3 by soot to be much less than a fraction of a percent. For example, we calculate values of $\Delta°G$ and K_p to be -11.4 kcal mol^{-1} and 2.2×10^{11} atm^{-1} for a 90% coverage, where the entropy change is estimated to be ~ -21 cal mol^{-1}. If the coverage is increased above 90%, entropy changes due to configuration become significant. In other words, at higher coverage, we derive a more negative entropy change and consequently a lesser negative $\Delta°G$ and a lower value of K_p. Even under these high coverage conditions, the HNO_3 uptake by carbonaceous aerosol would be negligibly small. Baumgardner et al.[10] have measured up to 200 ng m^{-3} of BC in the Arctic lower stratosphere above 9 km. We estimate the surface area of this loading to be $\sim 2 \times 10^{-8}$ cm^2 cm^{-3}. On such surfaces, even for a 100% coverage, the fractional removal of HNO_3 from the UTLS region would be much smaller than that calculated above for processed BC in the urban region. We should note, however, that the conclusion regarding HNO_3 removal could be altered if soot is modified in the atmosphere during its residence. Therefore, uptake measurements on atmospheric soot would be beneficial.

Heterogeneous reactions involving nitric acid on the aerosol can take place. Also, there could be enhanced photolysis on soot surfaces. It may be important to determine the uptake of nitric acid on aerosols relevant to the troposphere and examine possible surface chemical processes.

Conclusions

Uptake of HNO_3 was studied on *n*-hexane soot at room temperature (295 K) and on TC-1 kerosene soot at 253, 273 and 295 K as a function of the concentration of HNO_3. The uptake is mostly reversible and does not produce any HONO, NO_2, NO_3 or N_2O_5. FTIR studies could not detect any bound HNO_3 on the soot surface at room temperature. We could not detect any organic nitrate on the surface of the soot at partial pressure of HNO_3 up to 3×10^{-4} Torr at a flow rate of 30 sccm He over a period of 30 min. From the uptake measurements, the heat of adsorption has been determined to be -10.8 ± 2.1 kcal mol^{-1} averaged over the entire coverage range in our experiment (<12% of monolayer). But for soot surfaces, it is more appropriate to use isosteric heats of adsorption, which were determined to be -15.3 ± 1.0, -14.1 ± 0.5 and -13.4 ± 0.5 kcal mol^{-1} for 1.6%, 3.2% and 4.8% coverage, respectively. On the basis of the atmospheric concentrations of black carbon aerosol and HNO_3 abundance, HNO_3 adsorption on soot aerosol is not predicted to be significant. Therefore, we conclude that the uptake of HNO_3 on soot is not a significant loss process for HNO_3 unless it undergoes rapid reaction with another species or light.

Acknowledgment. This work is funded in part by NOAA's Air Quality Program and by CRDF under Project RC1-2327-MO-02 and Scientific School No 1713.2003.2. E.E.L. and O.B.P. gratefully acknowledge Dr. N. K. Shonija at Chemical Department of MSU for her kind support in measuring the surface area of soot and discussions.

References and Notes

(1) Lary, D. J.; Shallcross, D. E.; Toumi, R. *J. Geophys. Res.-Atmos.* **1999**, *104*, 15929.

(2) Horvath, H. *Atmos. Environ. Part a-Gen. Top.* **1993**, *27*, 293.
(3) Gorbunov, B.; Baklanov, A.; Kakutkina, N.; Windsor, H. L.; Toumi, R. *J. Aerosol Sci.* **2001**, *32*, 199.
(4) Brown, R. C.; MiakeLye, R. C.; Anderson, M. R.; Kolb, C. E.; Resch, T. J. *J. Geophys. Res.-Atmos.* **1996**, *101*, 22939.
(5) Schumann, U.; Strom, J.; Busen, R.; Baumann, R.; Gierens, K.; Krautstrunk, M.; Schroder, F. P.; Stingl, J. *J. Geophys. Res.-Atmos.* **1996**, *101*, 6853.
(6) Popovicheva, O. B.; Persiantseva, N. M.; Trukhin, M. E.; Rulev, G. B.; Shonija, N. K.; Buriko, Y. Y.; Starik, A. M.; Demirdjian, B.; Ferry, D.; Suzanne, J. *Phys. Chem. Chem. Phys.* **2000**, *2*, 4421.
(7) Popovicheva, O. B.; Persiantseva, N. M.; Lukhovitskaya, E. E.; Shonija, N. K.; Zubareva, N. A.; Demirdjian, B.; Ferry, D.; Suzanne, J. *Geophys. Res. Lett.* **2004**, *31*, doi 10.1029/2003GL018888.
(8) Pueschel, R. F.; Blake, D. F.; Snetsinger, K. G.; Hansen, A. D., A.; Verma, S.; Kato, K. *Geophys. Res. Lett.* **1992**, *19*, 1659.
(9) Baumgardner, D.; Kok, G.; Raga, G.; Diskin, G.; Sachse, G. W. *J. Aerosol Sci.* **2003**, *34*, 979.
(10) Baumgardner, D.; Kok, G.; Raga, G. *Geophys. Res. Lett.* **2004**, *31*, doi 10.1029/2003GL018883.
(11) Blake, D. F.; Kato, K. *J. Geophys. Res.-Atmos.* **1995**, *100*, 7195.
(12) Hendricks, J.; Kärcher, B.; Döpeleuer, A.; Feichter, J.; Lohmann, U.; Baumgardner, D. *Atmos. Chem. Phys.* **2004**, *4*, 2521.
(13) Cooke, W. F.; Wilson, J. J. N. *J. Geophys. Res.* **1996**, *101*, 19395.
(14) Aubin, D. G.; Abbatt, J. P. *J. Phys. Chem. A* **2003**, *107*, 11030.
(15) Kleffmann, J.; Wiessen, P. *Atmos. Chem. Phys.* **2005**, *5*, 77.
(16) Longfellow, C. A.; Ravishankara, A. R.; Hanson, D. R. *J. Geophys. Res.* **2000**, *105*, 24345.
(17) Saathoff, H.; Naumann, K.-H.; Reimer, N.; Kamm, S.; Mohler, O.; Schurath, U.; Vogel, H.; Vogel, B. *Geophys. Res. Lett.* **2001**, *28*, 1957.
(18) Disselkamp, R. S.; Carpenter, M. A.; Cowin, J. P. *J. Atmos. Chem.* **2000**, *37*, 113.
(19) Kirchner, U.; Scheer, V.; Vogt, R. *J. Phys. Chem. A* **2000**, *104*, 8908.
(20) Munoz, M. S. S.; Rossi, M. J. *Phys. Chem. Chem. Phys.* **2002**, *4*, 5110.
(21) Prince, A. P.; Wade, J. L.; Grassian, V. H.; Kleiber, P. D.; Young, M. A. *Atmos. Environ.* **2002**, *36*, 5729.
(22) Rogaski, C. A.; Golden, D. M.; Williams, L. R. *Geophys. Res. Lett.* **1997**, *24*, 381.
(23) Danilin, M. Y.; Fahey, D. W.; Schumann, U.; Prather, M. J.; Penner, J. E.; Ko, M. K. W.; Weisenstein, D. K.; Jackman, C. H.; Pitari, G.; Kohler, I.; Sausen, R.; Weaver, C. J.; Douglass, A. R.; Connell, P. S.; Kinnison, D. E.; Dentener, F. J.; Fleming, E. L.; Berntsen, T. K.; Isaksen, I. S. A.; Haywood, J. M.; Karcher, B. *Geophys. Res. Lett.* **1998**, *25*, 3947.
(24) Strawa, A. W.; Drdla, K.; Ferry, G. V.; Verma, S.; Pueschel, R. F.; Yasuda, M.; Salawitch, R. J.; Gao, R. S.; Howard, S. D.; Bui, P. T.; Loewenstein, M.; Elkins, J. W.; Perkins, K. K.; Cohen, R. *J. Geophys. Res.-Atmos.* **1999**, *104*, 26753.
(25) Longfellow, C. A.; Ravishankara, A. R.; Hanson, D. R. *J. Geophys. Res.-Atmos.* **1999**, *104*, 13833.
(26) Talukdar, R. K.; Gierczak, T.; McCabe, D. C.; Ravishankara, A. R. *J. Phys. Chem. A* **2003**, *107*, 5021.
(27) Smith, D. M.; Chutgai, A. R. *Colloids. Surf. A* **1995**, *105*, 47.
(28) Huey, L. G.; Hanson, D. R.; Howard, C. J. *J. Phys. Chem.* **1995**, *99*, 5001.
(29) Longfellow, C. A.; Imamura, T.; Ravishankara, A. R.; Hanson, D. R. *J. Phys. Chem. A* **1998**, *102*, 3323.
(30) Brown, R. L. *J. Res. Natl. Bur. Stand. U.S.* **1978**, *83*, 1.
(31) Howard, C. J. *J. Phys. Chem.* **1979**, *83*, 3.
(32) Nelsen, F. M.; Eggertsen, F. T. *Anal. Chem.* **1958**, *30*, 1387.
(33) Choi, W.; Leu, M.-T. *J. Phys. Chem. A* **1998**, *102*, 7618.
(34) Patrick, R.; Golden, D. M. *Int. J. Chem. Kinet.* **1983**, *15*, 1189.
(35) Adamson, A. W. *Physical Chemistry of Surfaces*, 4th ed.; John Wiley & Sons: New York, 1982.
(36) Kemball, C. *Proc. R. Soc., London, A* **1946**, *187*, 73.
(37) Kemball, C.; Rideal, E. K. *Proc. R. Soc., London, A* **1946**, *187*, 53.
(38) Talukdar, R. K.; Ravishankara, A. R. Uptake of N_2O_5 on aviation kerosene soot. To be published.
(39) Saathoff, H.; Naumann, K. H.; Riemer, N.; Kamm, S.; Mohler, O.; Schurath, U.; Vogel, H.; Vogel, B. *Geophys. Res. Lett.* **2001**, *28*, 1957.